

# Terrain Adaptive Odometry for Mobile Skid-steer Robots

Michal Reinstein, Vladimir Kubelka, Karel Zimmermann

**Abstract**—This paper proposes a novel approach to improving precision and reliability of odometry of skid-steer mobile robots by means inspired by robotic terrain classification (RTC). In contrary to standard RTC approaches we do not provide human labeled discrete terrain categories but we classify the terrain directly by the values of coefficients correcting the robot's odometry. Hence these coefficients make the odometry model adaptable to the terrain type due to inherent slip compensation. Estimation of these correction coefficients is based on feature extraction from the vibration data measured by an inertial measurement unit and regression function trained offline. Statistical features from the time domain, frequency domain, and wavelet features were explored and the best were automatically selected. To provide ground truth trajectory for the purpose of offline training a portable overhead camera tracking system was developed. Experimental evaluation on rough outdoor terrain proved  $67.9 \pm 7.5\%$  improvement in RMSE in position with respect to a state of the art odometry model. Moreover, our proposed approach is straightforward, easy for online implementation, and low on computational demands.

## I. INTRODUCTION

The ability of an autonomous mobile robot to traverse a complex and structured real world terrain is given by the means how much precise and reliable position and orientation information the robot has. Hence, improving the precision and reliability of navigation and localization algorithms is today still a relevant topic, especially in the field of mobile skid-steer robots performing outdoor missions. There are many different approaches to navigation and localization and their nature as well as performance is mostly determined by the sensor suit the robot is equipped with. Among the most common we can find approaches exploiting the inertial sensors (three accelerometers and three angular rate sensors mounted as an inertial measurement unit - IMU) [1] [2] [3] [4] [5] [6] [7], monocular [8] or stereo-camera [9] to compute visual odometry, laser scanners to provide range data [10] [11], barometer for height correction [12], and wheel odometry exploiting robot morphology conforming to uneven terrain [13]. Concerning the area of skid-steer robots it is actually the odometry that is most commonly exploited. With the research aiming primarily on slip estimation [2] [14] [4] [3], odometry proves to be crucial especially for rough terrain outdoor navigation. Therefore, we claim that by providing a

more precise and reliable odometry we can actually aid all these different approaches. Hence, seeking this improvement was our main motivation. Figure 1 shows the robotic platform used for outdoor experimental evaluation.



Figure 1. The mobile robot developed for the NIFTi ([www.nifti.eu](http://www.nifti.eu)) project; hardware design by BlueBotics ([www.bluebotics.com](http://www.bluebotics.com)), sensors equipped: Point Grey Ladybug 3 camera, rotating 2D laser scanner SICK LMS-151, Xsens MTI-G unit

It is generally well known that odometry of skid-steer robots is strongly affected by the environment especially by the terrain type. Complex structured, rough, or slippery terrain can cause the odometry to drift due to accumulation of uncompensated error or fail completely, when the speed of tracks or wheels ceases to correspond to the body velocity. As argued in [15], this can be solved by robotic terrain classification (RTC) that has become an increasingly active field of research in the last years [15]. Hand in hand with RTC goes the research into adaptive navigation realized either by means of changing the robot's morphology [16] or by selecting proper navigation strategy based on traversability analysis [17]. There has been lots of effort invested into the RTC methods lately [18], aiming mainly on identifying the terrain type and thus allowing a mobile robot to avoid dangerous regions or choose among suitable control modes. This leads to terrain dependent control as described in [18] where the reaction-base terrain classification subjected to the problem of speed and load dependency [18] [19] is addressed and solution via Singular Value Decomposition Interpolation is presented. As proposed in [15], identifying the terrain can also aid in localization and mapping by adjusting the location estimator based on characteristics of the identified terrain. Various approaches to the RTC problem also include support vector machines [20] [21], physical probabilistic models [22], neural networks [18] [23] [24], linear discriminant analysis [25] [26], principal component analysis [27] [28], or adaptive bayesian filtering [29]. Many approaches exploit both the vision and vibration measurements [30] [27], however these combined approaches tend to be rather computationally demanding.

Manuscript received 13. 9. 2012. M. Reinstein was supported by the project PRoViScout FP7-SPACE-241523, V. Kubelka by the project FP7-ICT-247870 NIFTi, and K. Zimmermann by the project P103/11/P700.

M. Reinstein is with the Department of Cybernetics, Faculty of Electrical Engineering, Czech Technical University in Prague, Prague, 166 27 Czech Republic (e-mail: [reinstein.michal@fel.cvut.cz](mailto:reinstein.michal@fel.cvut.cz)).

V. Kubelka is student at the Faculty of Electrical Engineering, Czech Technical University in Prague, (e-mail: [kubelvla@fel.cvut.cz](mailto:kubelvla@fel.cvut.cz)).

K. Zimmermann is with the Department of Cybernetics, Faculty of Electrical Engineering, Czech Technical University in Prague, Prague, 166 27 Czech Republic (e-mail: [zimmerk@cmp.felk.cvut.cz](mailto:zimmerk@cmp.felk.cvut.cz)).

Vast majority of these terrain classification approaches aims on correct labeling of the identified terrain types in the manner as perceived by humans. On the contrary, we claim that rather than labeling the terrain categories by human means it is more important to find representation that can be directly exploited by the robot, i.e. find terrain type representation by means essential for the robot. Sometimes, the same terrain type behaves differently under various circumstances (such as pebbles on flat terrain and pebbles on steep or uneven terrain) as well as different terrains can influence robot's odometry in a very similar way. In this way we diverge from the RTC concept since we do not appoint discrete labels to different terrain types. Our solution is based on the concept of sensing through body dynamic as described in [31] and successfully applied in our previous work concerning odometry for legged robots [32]. Although the skid-steer robot's morphology is completely different from the quadruped robot, the inertial sensors capture the body dynamics and its interaction with the environment in the same way. Therefore, we have modified a state of the art odometry model described in [3] and extended this model by additional two parameters—the correction coefficients. One of the coefficients is obtained by offline calibration and remains constant. The second is estimated using regression function trained on features computed on the vibration data measured by an IMU and changes adaptively to the terrain type. Feature selection was performed on a large and rich set of statistical time domain features, frequency domain features, and wavelet based features. When viewed from the RTC point of view, ranges of correction coefficients in fact correspond to terrain types that have very similar properties influencing the body dynamics. In this way, if the training data cover a sufficiently rich set of terrains, the slip is successfully compensated and precision of odometry improves.

Our main contribution lies in improving the traditional approach to odometry for skid-steer robots by proposing a RTC inspired machine learning method for estimating corrections. These corrections increase the precision of odometry even on rough outdoor terrain while the algorithm for computing the corrections is fast and easy to implement. However, offline training is required. We have trained and tested our approach on a set of 26 navigation experiments in total length 1762 m distance driven over 2.4 hours on rough outdoor terrain. For the evaluation we have taken a cross-validation approach where for each iteration the training dataset consisted of 20 randomly selected experiments leaving 6 experiments for testing. Precise reference trajectory was obtained using portable overhead camera and tracking system designed for this purpose. We have included our terrain adaptive odometry as one of the inputs to the navigation system of our robot and implemented it in the Robot Operating System (ROS). This navigation system is based on our previous work on complementary filter for orientation estimation using inertial sensors only [33] and provides full 3D position, velocity, and orientation.

The structure of this paper is as follows. Section II covers description of the proposed odometry model as well as methodology for feature extraction and training of the regression function. Section III provides details regarding the mobile robot and description of experiments. Section IV gives an overview of implications of our work.

## II. THEORY AND METHODOLOGY

### A. Enhanced Odometry Model with Correction Coefficients

Our approach is based on a track slip compensating odometry proposed by Endo [3] and modified by Nagatani [34]. The geometry of the odometry is depicted in Figure 2.

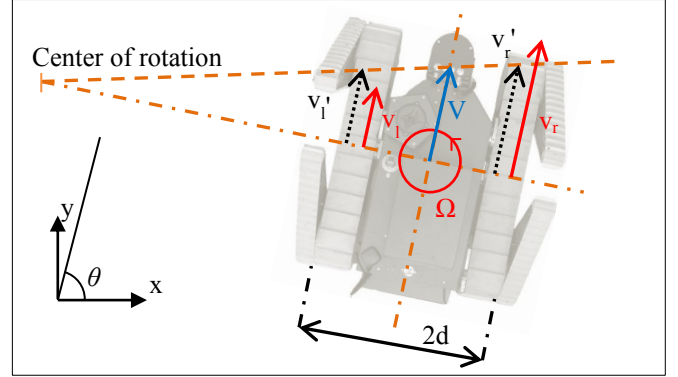


Figure 2. Geometry of the original odometry as proposed in [3] and modified in [34]. The different track velocities (measured  $v_l, v_r$ ; absolute  $v_l', v_r'$ ) cause the robot to follow a circular path around its Center of Rotation (CoR) with a tangential velocity  $V$  and to spin around its  $z$  axis (pointing upwards) with angular rate  $\Omega$  and heading  $\theta$  (after [34], Figure 2)

The track slip compensating odometry differential equations describing the coordinates are:

$$\dot{x} = \frac{v_r(1-a_r)+v_l(1-a_l)}{2} \cos \theta \quad (1a)$$

$$\dot{y} = \frac{v_r(1-a_r)+v_l(1-a_l)}{2} \sin \theta \quad (1b)$$

$$\dot{\theta} = \frac{v_r(1-a_r)-v_l(1-a_l)}{2d} \quad (1c)$$

where  $v_l$  and  $v_r$  are the left and right track velocities measured by internal sensors,  $2d$  is the distance between the tracks,  $\theta$  is heading such that  $\Omega = \dot{\theta}$ , and  $a_r, a_l$  are slip ratios defined as:

$$a_l = \frac{v_l - v_l'}{v_l} \quad (2a)$$

$$a_r = \frac{v_r - v_r'}{v_r} \quad (2b)$$

where  $v_l'$  and  $v_r'$  are the true velocities of the track gears moving through the coordinate frame. To determine  $a_r, a_l$  uniquely following equation can be used [34]:

$$\frac{a_l}{a_r} = -\text{sgn}(v_l \cdot v_r) \sqrt{\frac{v_r}{v_l}} \quad (3)$$

Combined with (1c), the slip ratios can be determined uniquely since  $\Omega = \dot{\theta}$  can be measured directly using the vertical axis angular rate sensor.

Our approach updates  $\theta$  using angular rate sensor measurements, which are corrected for bias and scale errors (4). The bias is determined during an initial calibration sequence; the scale factor is determined experimentally as an optimal parameter minimizing the localization error over a set of training experiments in a least squares sense.

$$\Omega_{cal} = S_{\Omega}(\Omega_{meas} - b_{\Omega}) \quad (4)$$

where  $\Omega_{cal}$  is the calibrated angular rate measurement,  $\Omega_{meas}$  is the measured one,  $S_{\Omega}$  and  $b_{\Omega}$  are the scale and bias,

respectively. To update the  $x$  and  $y$  coordinates, the  $a_r, a_l$  slip ratios are evaluated and substituted into (1a) and (1b). The position increments in these coordinates are subsequently multiplied by the correction coefficient  $C$  estimated using trained regression function:

$$\Delta x_{k-1}^k = \frac{\dot{x}_{k-1} + \dot{x}_k}{2} T_s C \quad (5a)$$

$$\Delta y_{k-1}^k = \frac{\dot{y}_{k-1} + \dot{y}_k}{2} T_s C \quad (5b)$$

where  $\Delta y_{k-1}^k$  and  $\Delta x_{k-1}^k$  stand for increments in position between discrete time steps  $k$  and  $k-1$ ,  $\dot{x}$  and  $\dot{y}$  are results of (1a,b) at the appropriate discrete time steps, and  $T_s$  is the sampling period.

These corrected position increments are then used to update the current position. Note that the correction coefficient changes only norm of the increment, not direction. Direction is believed to be accurate enough due to the angular rate measurement and scale factor calibration. Figure 3 demonstrates the correction coefficient  $C$  and the angular rate calibration effects on a trajectory.

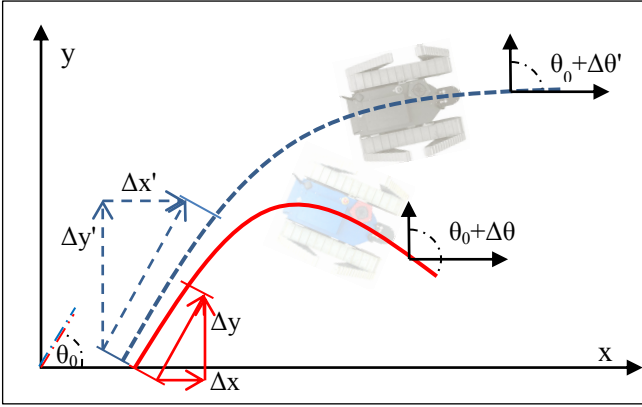


Figure 3. The ground truth path (blue dashed) and the odometry output (red solid). The goal of our approach is to diminish differences between position  $x, y$  and angle  $\theta$  increments.

### B. Regression Function Training

To estimate the correction coefficient as defined in (5a,b), we have chosen a straightforward yet sufficient approach of training a linear regression function  $C(x; \alpha)$ , which processes features obtained from inertial data (three accelerations and three angular rates at 90 Hz) and outputs the correction coefficient directly. It is given as follows:

$$C(x; \alpha) = \sum_{i=0}^n \alpha_i x_i \quad (6)$$

where  $n$  is the number of features,  $x_i$  is feature value,  $\alpha_i$  is corresponding parameter of the regression function,  $x_0 = 1$  is the intercept term.

Training of the regression function was performed using normal equations corresponding to minimization of the following cost function  $J(\alpha)$  in a least squares sense:

$$J(\alpha) = \frac{1}{2m} \sum_{k=1}^m (C(x^k; \alpha) - y^k)^2 \quad (7)$$

where  $m$  is the number of training examples,  $y^k$  is the correction coefficient obtained from the ground truth trajectory reference for the  $k^{th}$  training example.

The ground truth correction coefficients  $y^k$  were computed by offline local optimization in such a way to ensure that the trajectory obtained using the proposed model parameterized by these  $y^k$  coefficients coincides with the reference.

### C. Feature Extraction and Selection

Inspired by the feature pools used and analyzed in [15] [18] [20] we have decided to perform feature selection on the following features:

- features from the time defined as various statistical moments and indicators such as *min, max, mean, median, norm, skewness, kurtosis*, and number of sign changes over a threshold given by 0.25, 0.5, 0.75 multiples of *mean* and *median*,
- features from the frequency domain computed using FFT and taking into account the magnitudes and frequencies of first three most significant harmonics,
- features defined as correlation coefficient between the signal samples and more than a hundred of Haar wavelets generated with the corresponding length.

The feature selection was performed offline as part of the regression function training. We selected a set of suitable features from the generated feature pool by a forward stage-wise feature selection strategy [35] based on Gram-Schmidt orthogonalization process. More formally, we are given a training set  $\{x^1, y^1, \dots, x^k, y^k\}$  consisting of  $K$  training samples, where  $x^k, k = 1 \dots K$  are  $N$ -dimensional vectors containing values of features from the feature pool, and  $y^k$  are ground truth values of corresponding correction coefficients. Especially, we denote  $x_j^k$  as the  $j$ -th feature of the  $k$ -th sample.

The proposed algorithm successively builds the feature set from the features minimizing the residuals  $\Delta y^k$  of all training samples  $i = 1 \dots K$ . Initially we set residual of the  $k$ -th training sample to  $\Delta y^k = y^k$ . In each training stage  $h$ , the algorithm estimates coefficients for all features  $j = 1 \dots N$

$$a_j = \frac{\sum_i \Delta y^k x_j^k}{\sum_k x_j^k x_j^k} \quad (8)$$

We choose the feature with index  $i = \arg \min_j r(j)$ , which minimize square error

$$r(j) = \sum_k (a_j x_j^k - \Delta y^k)^2 \quad (9)$$

Eventually, we set coefficient of the feature selected in stage  $h$  to  $\alpha_h = a_i$  and update residuals  $\Delta y^k = \Delta y^k - \alpha_h x_i^k$ . The algorithm continues while the validation error is decreasing or a given number of features to be selected have been reached.

## III. EVALUATION AND RESULTS

### A. Robotic Platform Description

Our experimental platform used for verification is a skid-steer robot (see Figure 1) designed for urban search and rescue operations and developed as part of a project aiming at human-robot cooperation in dynamic environments. For purpose of our experiments we used the Xsens MTi-G unit

providing calibrated and temperature compensated inertial data at 90 Hz in range of  $\pm 300$  deg/s and  $\pm 50$  m/s<sup>2</sup> for angular rates and accelerations respectively, and motor encoders providing left and right track velocities at 20 Hz. We have collected datasets on various outdoor terrains (paving, asphalt, concrete, stones, pebbles, sand, dust, soil, and grass) to test the limits under natural conditions. The robot was teleoperated during these experiments and tracked using overhead camera and video tracking system we have developed for this purpose. We tracked the robot's position and heading in time by exploiting two distinct markers as shown in Figure 4 (left). Then we projected the tracked trajectory into the metric plane of motion determined as part of the calibration of the tracking system. This way we were able to obtain a sufficiently precise 2D referential trajectory. The position accuracy of the reference was determined experimentally to be  $15 \pm 12$  cm within the  $15 \text{ m} \times 10 \text{ m}$  area; example is shown in Figure 4 (right). For data collection and testing, different areas were used.

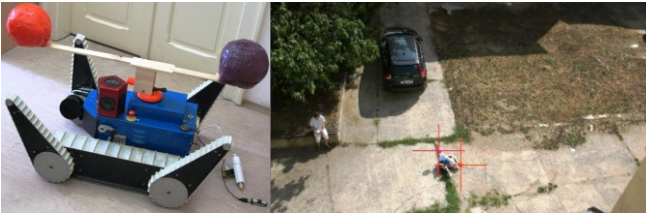


Figure 4. The mobile robotic platform equipped with colored markers for position and heading tracking (left); example of one of the testing areas as processed by the tracking algorithm (right).

### B. Evaluation and Testing

We have performed a number of experiments to test and evaluate our approach. First, we determined the optimal number of inertial data samples to be used for computing the features. We iterated over the validation dataset for different numbers of samples in range of 10 to 400 and observed the error on the training dataset. This way the optimal number of samples was determined to be 98. For the real-time online implementation this means: each time a new odometry measurement comes at 20Hz, from that time step the 98 last samples of the 6 inertial signals (sampled at 90 Hz) are processed to compute the features.

Second, another series of experiments was carried out to determine the optimal number of features to be selected during the proposed feature selection procedure. Again, we iterated over the whole validation dataset and for different numbers of features in range 1 to 100 we assessed the RMSE precision of the corrected trajectory with respect to reference and the possible computational load for online computation of the features. This proved that using only the best 20 features is fully sufficient. Among the top 20 features, which contributed the most to decreasing of the validation error during the feature selection procedure, most of them were from the group of statistical time domain features. These features proved to be the best for capturing information about changes in motion dynamics corresponding to disturbances to the proposed odometry model caused by the nature of terrain.

Third, to field-test our algorithm and evaluate the desired improvement in precision of navigation, we compared the development of RMSE in time of our approach (with respect

to the ground truth trajectory) to the RMSE development of the trajectory obtained using the original odometry model [3]. To avoid being biased by the choice of the training and testing datasets, we performed a thorough cross-validation of more than 1000 iterations over all of the navigation experiments. For each cross-validation check we have randomly selected 20 trajectories for training the regression function and the remaining 6 trajectories were used for testing, i.e. evaluation of the RMSE in time with respect to the reference. To visualize our results, we have selected two typical samples of navigation trajectories. One represents a short trajectory (chosen for convenience of plotting); see Figure 5 showing the correction coefficients evaluated on testing dataset corresponding to trajectory shown in Figure 6. Second trajectory represents a longer and more dynamic experiment; see Figure 7. Both navigation experiments were taken on a rough outdoor terrain consisting of combination of concrete with sand, soil, grass, and stones.

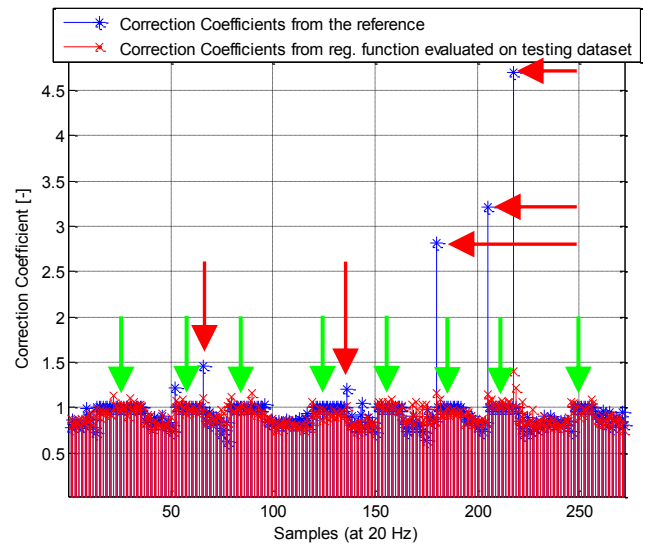


Figure 5. Example of evaluation of the trained regression function on a testing dataset—navigation experiment described in Figure 6): ground truth coefficients as obtained from the reference (blue), coefficients computed on the testing data (red). Red arrows point to uncompensated corrections—outlying cases not covered by the training data; green arrows point approximately to the regions of correction coefficients = 1 meaning almost no corrections were necessary.

As shown in Figure 5, the regression function was capable of estimating reliable correction coefficients for vast majority of the samples. However, as highlighted by the red arrows, in few outlying cases, the correction was underestimated. This was very probably caused by the diverse nature of the outdoor terrain, which was not fully covered in the training dataset. Although we can never possibly capture such training dataset to cover a complete response of the robot's body dynamics to the terrain, we show that even when trained on ground of different properties, our approach provides desired results. As also shown in Figure 5 and highlighted by green arrows, there were samples for which the correction coefficients became close to 1, meaning only very small correction was necessary, and the regression function did respect this correctly.

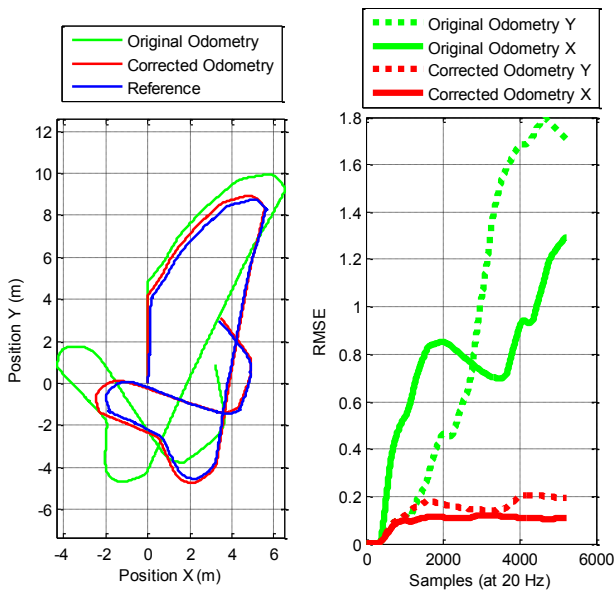


Figure 6. Example of short trajectory navigation experiment: comparison of performance of the original odometry model as described in [3] and our approach (left) with respect to the reference; development of RMSE in position in time for original odometry model and corrected model (right).

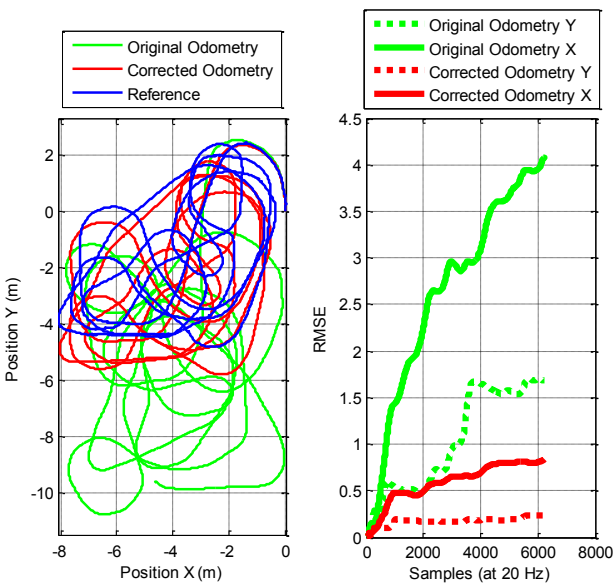


Figure 7. Example of long trajectory navigation experiment: comparison of performance of the original odometry model as described in [3] and our approach (left) with respect to the reference; development of RMSE in position in time for original odometry model and corrected model (right).

Figure 6 (right) and Figure 7 (right) show how the RMSE in position grows in time for both the original odometry model [3] and our model with terrain adaptive corrections. Although the improvement is as desired, it is important to note that the odometry is still dead reckoning navigation and hence the error grows inevitably with the distance driven. To conclude, for the evaluation we have gathered more than 2.4 hours of data and driven more than 1762 m. The overall average improvement in precision of navigation over all of the 26 cross-validated experiments was  $67.9 \pm 7.5\%$  of the RMSE with respect to the original odometry model proposed in [3].

#### IV. CONCLUSION

Motivated by the successful development in the field of RTC during last years and the work done on improving odometry models for skid-steer robots, we propose a modification of the state of the art odometry model described in [3] making it adaptable to the terrain. We propose such a parameterization of the odometer model that one constant parameter modifies the vertical gyro scale factor (identified by experimental calibration) and the second parameter changes adaptively with the terrain the robot is driving over. We show this can be achieved in a straightforward and easy to implement way by computing features on six inertial signals obtained from an IMU at sufficiently high rate. These features then enter a regression function trained to directly output the adaptive correction coefficient. We have proven that just by using 20 best features computed over 98 samples of inertial data the average improvement of  $67.9 \pm 7.5\%$  was achieved in the RMSE in position with respect the original uncorrected model [3]. To avoid being biased by the choice of the testing and training datasets we performed a thorough cross-validation.

We are fully aware that due to rather large diversity of properties of different terrain types the performance of our approach will always depend upon the actual choice of the training dataset as well as on the dynamics of motion. Training the regression function indoor will not improve much the outdoor performance as well as driving at completely different speeds during training and testing. On the other hand, when trained on indoor data, improvement in precision of indoor navigation will be even more significant since the response of body dynamics to the indoor terrain is much more consistent and the correction coefficients will be estimated more precisely.

We assume this work can easily be extended by processing images from robot's omnicaamera by means of segmenting visually consistent ground regions and assigning to them ranges of the correction coefficients. Since the robot can create a map using the laser scanner the information about how each terrain type influences the precision of the odometry model can be directly projected to this map leading to a more convenient trajectory planning.

#### V. ACKNOWLEDGEMENT

This work was supported by the following projects: FP7-SPACE-241523 PRoViScout, FP7-ICT-247870 NIFTi, and GACR P103/11/P700.

#### REFERENCES

- [1] T. Yoshida, K. Irie, E. Koyanagi and M. Tomono, "A sensor platform for outdoor navigation using gyro-assisted odometry and roundly-swinging 3D laser scanner," in *Proc. IEEE/RSJ Int Intelligent Robots and Systems (IROS) Conf.*, 2010.
- [2] J. Yi, J. Zhang, D. Song and S. Jayasuriya, "IMU-based localization and slip estimation for skid-steered mobile robots," in *Proc. IEEE/RSJ Int. Conf. Intelligent Robots and Systems IROS 2007*, 2007.
- [3] D. Endo, Y. Okada, K. Nagatani and K. Yoshida, "Path following control for tracked vehicles based on slip-compensating odometry," in *Proc. IEEE/RSJ Int. Conf. Intelligent Robots and Systems IROS 2007*, 2007.

- [4] P. Lamon and R. Siegwart, "Inertial and 3D-odometry fusion in rough terrain - towards real 3D navigation," in *Proc. IEEE/RSJ Int. Conf. Intelligent Robots and Systems (IROS 2004)*, 2004.
- [5] H. Wang, J. Zhang, J. Yi, D. Song, S. Jayasuriya and J. Liu, "Modeling and motion stability analysis of skid-steered mobile robots," in *Proc. IEEE Int. Conf. Robotics and Automation ICRA '09*, 2009.
- [6] D. Hyun, H. S. Yang, G. H. Yuk and H. S. Park, "A dead reckoning sensor system and a tracking algorithm for mobile robots," in *Proc. IEEE Int. Conf. Mechatronics ICM 2009*, 2009.
- [7] F. Azizi and N. Houshang, "Mobile robot position determination using data from gyro and odometry," in *Proc. Canadian Conf. Electrical and Computer Engineering*, 2004.
- [8] J. Shen, D. Tick and N. Gans, "Localization through fusion of discrete and continuous epipolar geometry with wheel and IMU odometry," in *Proc. American Control Conf. (ACC)*, 2011.
- [9] S. A. Rodriguez F, V. Fremont and P. Bonnifait, "An experiment of a 3D real-time robust visual odometry for intelligent vehicles," in *Proc. 12th Int. IEEE Conf. Intelligent Transportation Systems ITSC '09*, 2009.
- [10] Y. Zhuang, S. Yang, X. Li and W. Wang, "3D-laser-based visual odometry for autonomous mobile robot in outdoor environments," in *Proc. 3rd Int Awareness Science and Technology (iCAST) Conf*, 2011.
- [11] T. Suzuki, M. Kitamura, Y. Amano and T. Hashizume, "6-DOF localization for a mobile robot using outdoor 3D voxel maps," in *Proc. IEEE/RSJ Int Intelligent Robots and Systems (IROS) Conf*, 2010.
- [12] Y. Morales, T. Tsubouchi and S. Yuta, "Vehicle 3D localization in mountainous woodland environments," in *Proc. IEEE/RSJ Int. Conf. Intelligent Robots and Systems IROS 2009*, 2009.
- [13] G. Ishigami, E. Pineda, J. Overholt, G. Hudas and K. Iagnemma, "Performance analysis and odometry improvement of an omnidirectional mobile robot for outdoor terrain," in *Proc. IEEE/RSJ Int Intelligent Robots and Systems (IROS) Conf*, 2011.
- [14] A. Sakai, Y. Tamura and Y. Kuroda, "An efficient solution to 6DOF localization using Unscented Kalman Filter for planetary rovers," in *Proc. IEEE/RSJ Int. Conf. Intelligent Robots and Systems IROS 2009*, 2009.
- [15] D. Tick, T. Rahman, C. Busso and N. Gans, "Indoor robotic terrain classification via angular velocity based hierarchical classifier selection," in *Proc. IEEE Int Robotics and Automation (ICRA) Conf*, 2012.
- [16] D. Chugo, K. Kawabata, H. Kaetsu, S. Jia, H. Asama, T. Mishima and K. Takase, "3D Odometry based on body configuration," in *Proc. SICE Annual Conf*, 2008.
- [17] A. Howard and H. Seraji, "Real-time assessment of terrain traversability for autonomous rover navigation," in *Proc. IEEE/RSJ Int. Conf. Intelligent Robots and Systems (IROS 2000)*, 2000.
- [18] E. Coyle, E. G. Collins and R. G. Roberts, "Speed independent terrain classification using Singular Value Decomposition Interpolation," in *Proc. IEEE Int Robotics and Automation (ICRA) Conf*, 2011.
- [19] E. G. Collins and E. J. Coyle, "Vibration-based terrain classification using surface profile input frequency responses," in *Proc. IEEE Int. Conf. Robotics and Automation ICRA 2008*, 2008.
- [20] C. Weiss, H. Frohlich and A. Zell, "Vibration-based Terrain Classification Using Support Vector Machines," in *Proc. IEEE/RSJ Int Intelligent Robots and Systems Conf*, 2006.
- [21] I. Halatci, C. A. Brooks and K. Iagnemma, "Terrain Classification and Classifier Fusion for Planetary Exploration Rovers," in *Proc. IEEE Aerospace Conf*, 2007.
- [22] K. Iagnemma, F. Genot and S. Dubowsky, "Rapid physics-based rough-terrain rover planning with sensor and control uncertainty," in *Proc. IEEE Int Robotics and Automation Conf*, 1999.
- [23] R. Jitpakdee and T. Maneewarn, "Neural networks terrain classification using Inertial Measurement Unit for an autonomous vehicle," in *Proc. SICE Annual Conf*, 2008.
- [24] P. Giguere and G. Dudek, "A Simple Tactile Probe for Surface Identification by Mobile Robots," *IEEE Transactions on Robotics*, vol. 27, no. 3, pp. 534-544, 2011.
- [25] C. A. Brooks and K. Iagnemma, "Vibration-based terrain classification for planetary exploration rovers," *IEEE Transactions on Robotics*, vol. 21, no. 6, pp. 1185-1191, 2005.
- [26] C. Brooks, K. Iagnemma and S. Dubowsky, "Vibration-based Terrain Analysis for Mobile Robots," in *Proc. IEEE Int. Conf. Robotics and Automation ICRA 2005*, 2005.
- [27] K. Iagnemma, C. Brooks and S. Dubowsky, "Visual, tactile, and vibration-based terrain analysis for planetary rovers," in *Proc. IEEE Aerospace Conf*, 2004.
- [28] E. M. DuPont, C. A. Moore and R. G. Roberts, "Terrain classification for mobile robots traveling at various speeds: An eigenspace manifold approach," in *Proc. IEEE Int. Conf. Robotics and Automation ICRA 2008*, 2008.
- [29] P. Komma, C. Weiss and A. Zell, "Adaptive bayesian filtering for vibration-based terrain classification," in *Proc. IEEE Int. Conf. Robotics and Automation ICRA '09*, 2009.
- [30] C. Weiss, H. Tamimi and A. Zell, "A combination of vision- and vibration-based terrain classification," in *Proc. IEEE/RSJ Int. Conf. Intelligent Robots and Systems IROS 2008*, 2008.
- [31] F. Iida and R. Pfeifer, "Sensing through body dynamics," *Robotics and Autonomous Systems*, vol. 54, no. 8, pp. 631-640, 2006.
- [32] M. Reinstein and M. Hoffmann, "Dead reckoning in a dynamic quadruped robot: Inertial navigation system aided by a legged odometer," in *Proc. IEEE Int Robotics and Automation (ICRA) Conf*, 2011.
- [33] V. Kubelka and M. Reinstein, "Complementary filtering approach to orientation estimation using inertial sensors only," in *Proc. IEEE Int Robotics and Automation (ICRA) Conf*, 2012.
- [34] K. Nagatani, N. Tokunaga, Y. Okada and K. Yoshida, "Continuous Acquisition of Three-Dimensional Environment Information for Tracked Vehicles on Uneven Terrain," in *Proc. IEEE Int. Workshop Safety, Security and Rescue Robotics SSRR 2008*, 2008.
- [35] S. Weisberg, *Applied Linear Regression*, John Wiley & Sons, 2005.